



Response of the Anaerobic Methanotrophic Archaeon *Candidatus "Methanoperedens nitroreducens"* to the Long-Term Ferrihydrite Amendment

Chen Cai^{1,2}, Gaofeng Ni², Jun Xia², Xueqin Zhang², Yue Zheng³, Bingqing He^{2,4}, Esteban Marcellin⁴, Weiwei Li^{2,5}, Jiaoyang Pu², Zhiguo Yuan² and Shihu Hu^{2*}

OPEN ACCESS

Edited by:

Frank Schreiber,
Federal Institute for Materials
Research and Testing (BAM),
Germany

Reviewed by:

Joerg Stefan Deutzmann,
Stanford University, United States
Florin Musat,
Helmholtz Centre for Environmental
Research, Helmholtz Association
of German Research Centres (HZ),
Germany

*Correspondence:

Shihu Hu
s.hu@uq.edu.au

Specialty section:

This article was submitted to
Microbial Physiology and Metabolism,
a section of the journal
Frontiers in Microbiology

Received: 22 October 2021

Accepted: 10 March 2022

Published: 18 April 2022

Citation:

Cai C, Ni G, Xia J, Zhang X,
Zheng Y, He B, Marcellin E, Li W,
Pu J, Yuan Z and Hu S (2022)
Response of the Anaerobic
Methanotrophic Archaeon
*Candidatus "Methanoperedens
nitroreducens"* to the Long-Term
Ferrihydrite Amendment.
Front. Microbiol. 13:799859.
doi: 10.3389/fmicb.2022.799859

¹ CAS Key Laboratory of Urban Pollutant Conversion, Department of Environmental Science and Engineering, University of Science and Technology of China, Hefei, China, ² Australian Centre for Water and Environmental Biotechnology, The University of Queensland, St Lucia, QLD, Australia, ³ State Key Laboratory of Marine Environmental Science, College of the Environment and Ecology, Xiamen University, Xiamen, China, ⁴ Australian Institute for Bioengineering and Nanotechnology, The University of Queensland, St Lucia, QLD, Australia, ⁵ State Key Laboratory of Coal Mine Disaster Dynamics and Control, Chongqing University, Chongqing, China

Anaerobic methanotrophic (ANME) archaea can drive anaerobic oxidation of methane (AOM) using solid iron or manganese oxides as the electron acceptors, hypothetically *via* direct extracellular electron transfer (EET). This study investigated the response of *Candidatus "Methanoperedens nitroreducens TS"* (type strain), an ANME archaeon previously characterized to perform nitrate-dependent AOM, to an Fe(III)-amended condition over a prolonged period. Simultaneous consumption of methane and production of dissolved Fe(II) were observed for more than 500 days in the presence of *Ca. "M. nitroreducens TS,"* indicating that this archaeon can carry out Fe(III)-dependent AOM for a long period. *Ca. "M. nitroreducens TS"* possesses multiple multiheme *c*-type cytochromes (MHCs), suggesting that it may have the capability to reduce Fe(III) *via* EET. Intriguingly, most of these MHCs are orthologous to those identified in *Candidatus "Methanoperedens ferrireducens,"* an Fe(III)-reducing ANME archaeon. In contrast, the population of *Ca. "M. nitroreducens TS"* declined and was eventually replaced by *Ca. "M. ferrireducens,"* implying niche differentiation between these two ANME archaea in the environment.

Keywords: anaerobic oxidation of methane, Fe(III) reduction, ANME archaea, extracellular electron transfer, multiheme *c*-type cytochromes, methanogen, acetate

INTRODUCTION

Anaerobic oxidation of methane (AOM) occurs in a wide range of natural and anthropogenic environments and plays a crucial role in mitigating the global emission of methane by converting this greenhouse gas to less potent CO₂ (Knittel and Boetius, 2009). In marine settings, AOM contributes to consuming >90% of the methane produced *via* methanogenesis, which makes the ocean a minor methane source (Hinrichs and Boetius, 2002; Reeburgh, 2007). AOM also

prominently controls methane flux in some non-marine environments (Hu et al., 2014; Segarra et al., 2015). It is estimated that AOM reduces over 50% of methane emissions in freshwater wetlands, the largest natural methane source (Segarra et al., 2015).

It has been well-documented that AOM can be coupled to the reduction of sulfate, nitrate, and nitrite (Welte et al., 2016; Bhattarai et al., 2019). These AOM processes are conducted by either anaerobic methanotrophic (ANME) archaea or NC10 bacteria (Knittel and Boetius, 2009; Ettwig et al., 2010). Theoretically, AOM coupling to Fe(III) reduction is also thermodynamically favorable. A number of recent incubation studies, in fact, have shown that some ANME species belonging to ANME-2 cluster are able to conduct Fe(III)-dependent AOM (Ettwig et al., 2016; Scheller et al., 2016; Cai et al., 2018; Li et al., 2021). *Candidatus "Methanoperedens ferrireducens,"* affiliated with family *Candidatus "Methanoperedenaceae"* (formerly ANME-2d), could use ferrihydrite as the electron acceptor in a long-term incubation (Cai et al., 2018). Intriguingly, a few other ANME-2 archaea using electron acceptors such as sulfate and nitrate also showed the capability to reduce Fe(III) (Ettwig et al., 2016; Scheller et al., 2016). For instance, *Candidatus "Methanoperedens nitroreducens TS"* (type strain) has been characterized to grow on nitrate (Haroon et al., 2013), while a *Ca. "M. nitroreducens"*-like archaeon (strain MPEBLZ) could perform Fe(III)-dependent AOM in the absence of nitrate (Ettwig et al., 2016). In addition, marine ANME-2 archaea normally mediate sulfate-dependent AOM in cooperation with sulfate-reducing bacteria (Knittel and Boetius, 2009). Using Fe(III) in substitution for sulfate, the ANME-2 archaea reduced Fe(III) without syntrophic interaction with their bacterial partners (Scheller et al., 2016).

It is hypothesized that ANME archaea catalyze Fe(III) reduction *via* extracellular electron transfer (EET; McGlynn et al., 2015; Ettwig et al., 2016; Scheller et al., 2016; Cai et al., 2018; Leu et al., 2020). In dissimilatory metal-reducing microorganisms such as *Geobacter* and *Shewanella*, EET is carried out *via* multiheme *c*-type cytochromes (MHCs; Shi et al., 2016). Likewise, metagenomic analyses revealed that ANME archaea harbor genes encoding numerous MHCs (Meyerdierks et al., 2010; Wang et al., 2014; McGlynn et al., 2015). The number and size of the MHCs in these ANME archaea are comparable to, or even larger than, those in metal-reducing bacteria (Shi et al., 2007; McGlynn et al., 2015; Cai et al., 2018; Leu et al., 2020). For instance, ANME-1 and ANME-2a archaea encode 11 (Meyerdierks et al., 2010) and 16 species (Wang et al., 2014; McGlynn et al., 2015) of MHCs, respectively. Members of *Ca. "Methanoperedenaceae"* encode larger numbers of MHCs (25–46 species) (Haroon et al., 2013; Ettwig et al., 2016; Cai et al., 2018; Leu et al., 2020). Intriguingly, some of the ANME species encode MHCs with a large number of hemes (e.g., a 113-heme MHC in *Candidatus "Methanoperedens manganioreducens"*) (Leu et al., 2020). Moreover, MHCs showed high expression levels concomitant with metal reduction by ANME archaea (Cai et al., 2018; Leu et al., 2020). Together, these results strongly suggest that MHCs of ANME archaea are involved in EET, which allows these microorganisms to respire metal oxides such as Fe(III).

Increasing geochemical studies have provided evidence that AOM can be driven by Fe(III) reduction in many aquatic environments (Beal et al., 2009; Crowe et al., 2011; Sivan et al., 2011; Amos et al., 2012; Wankel et al., 2012; Segarra et al., 2013; Riedinger et al., 2014; Egger et al., 2015; Egger et al., 2016). In fact, iron oxides are prevalent in freshwater bodies (Martin and Meybeck, 1979) and soils (Deshpande et al., 1964), and large amounts of iron (~730 Tg/year) are further transported from continents to oceans *via* rivers annually (Martin and Meybeck, 1979). These environments are also characterized as important methane sources and/or sinks (Topp and Pattey, 1997; Conrad, 2009; Knittel and Boetius, 2009). Thus, it can be predicted that Fe(III)-dependent AOM takes place in a variety of environments rich in iron and methane, making this bioprocess a methane sink with potential global importance.

For in-depth understanding of Fe(III)-dependent AOM in nature, it is critical to identify the indigenous microorganisms responsible for this process. A recent study, in fact, has reported that *Ca. "M. nitroreducens"*-like archaea exhibited AOM activity in an iron-rich, low-sulfate freshwater lake sediment (Weber et al., 2017). Furthermore, as aforementioned, Fe(III) reduction by *Ca. "M. nitroreducens MPEBLZ"* has been demonstrated (Ettwig et al., 2016). Thus, it is likely that *Ca. "M. nitroreducens TS"* or *Ca. "M. nitroreducens MPEBLZ"* are potential candidates for conducting Fe(III)-dependent AOM in the environment. However, evidence for these archaea to grow on Fe(III) condition is currently lacking (In 't Zandt et al., 2018).

The aim of this study was to investigate whether *Ca. "M. nitroreducens"* can adapt to a Fe(III)-amended condition over the long-term periods. An inoculum dominated by *Ca. "M. nitroreducens TS"* was seeded in a bioreactor amended with an environmentally relevant form of Fe(III) oxide (ferrihydrite) and incubated for 800 days. Notably, *Ca. "M. ferrireducens"* has been indicated to be an obligate methane-dependent Fe(III) reducer as it lacks nitrate reductase when compared to *Ca. "M. nitroreducens"* (Cai et al., 2018). Therefore, to facilitate an evaluation of the response of *Ca. "M. nitroreducens"* to the Fe(III) condition, the incubation conditions for *Ca. "M. ferrireducens"* were employed in this study (Cai et al., 2018). Bioreactor performance and microbial community were monitored throughout the incubation. Metagenomic analysis was performed to reveal the metabolic capacity of *Ca. "M. nitroreducens TS"* and other key microorganisms.

MATERIALS AND METHODS

Biomass Source

Biomass was originally from a culture dominated by *Ca. "M. nitroreducens TS"* (Haroon et al., 2013). In this study, the biomass was taken from a parent bioreactor performing nitrate-dependent AOM and anammox. The total volume of the parent bioreactor was 5.6 L, consisting of 4.6 L mixed biomass and 1.0 L headspace. The parent bioreactor was supplied with methane, nitrate, and ammonium and operated at $24 \pm 1^\circ\text{C}$ and neutral pH (7.0–7.5). At the time of biomass sampling for both short-term and long-term tests, the AOM rate of the parent bioreactor

was $301.1 \mu\text{M day}^{-1}$, along with a nitrate reduction rate of $1,130.6 \mu\text{M day}^{-1}$. It indicated that AOM was predominantly coupled to nitrate reduction, which was in line with the abundance of *Ca. "M. nitroreducens TS"* (~30%) in the microbial community. The nitrite-reducing methanotrophic bacterium (*Candidatus "Methylomirabilis oxyfera"*) only accounted for less than 1%, implying its contribution to methane oxidation was minimal. Ammonium was consumed by anammox bacterium (*Candidatus "Kuenenia stuttgartiensis"*) at a rate of $881.5 \mu\text{M day}^{-1}$, which accounted for the complete removal of nitrite produced by *Ca. "M. nitroreducens TS"*.

Short-Term Batch Tests

Metagenomic analysis showed that *Ca. "M. nitroreducens TS"* only shares an average nucleotide identity (ANI) of 77.4% with *Ca. "M. nitroreducens MPEBLZ"* (Supplementary Figure 3) (Arshad et al., 2015), which was demonstrated to perform Fe(III)-dependent AOM (Ettwig et al., 2016). Thus, it necessitates an assessment of the capability of *Ca. "M. nitroreducens TS"* to carry out this process. One 230 ml batch reactor (A1) was flushed with N_2 to remove oxygen. A1 was then inoculated with 100 ml biomass. Methane was supplied by sparging gas mix (90% CH_4 , 5% CO_2 , and 5% N_2) through the liquid phase for 3 min. The batch tests were conducted in two stages. In Stage I, residual nitrate in the inoculum was served as the electron acceptor for AOM. In Stage II, after nitrate was depleted, Fe(III) citrate (Sigma-Aldrich, United States) was added, as the sole electron acceptor, at a concentration of 4 mM. Another batch reactor (A2) was set up and operated identically to A1 as a control. However, sodium citrate (Sigma-Aldrich, United States), instead of Fe(III) citrate, was supplied to A2 in Stage II. Gas samples were taken every 1–3 days for methane and N_2 measurement. AOM rate equals the methane consumption rate, which was determined from the measured methane concentration through linear regression (Haroon et al., 2013). Nitrate was monitored using the test strips (Merck, Germany) until it was depleted in Stage I.

Incubation Under the Long-Term Ferrihydrite Amendment

To evaluate the response of *Ca. "M. nitroreducens TS"* to the Fe(III) condition in a long-term period, a bioreactor was inoculated with biomass and supplied with Fe(III) in the form of ferrihydrite as the sole electron acceptor. In total, 300 ml biomass was mixed with 600 ml medium in a 1.1 L bioreactor using a magnetic stirrer at 300 rpm. The bioreactor was operated at $24 \pm 1^\circ\text{C}$ and neutral pH.

The entire incubation period was divided into two stages. In Stage I (Days 0–47), the bioreactor was supplied with nitrate as the electron acceptor for AOM. Methane was replenished by flushing the bioreactor with a gas mix (90% CH_4 , 5% CO_2 , and 5% N_2) every 1–2 weeks. Gas samples were taken daily for methane measurement, and liquid samples were taken two times each week for nitrate, nitrite, and ammonium measurement. AOM rate was determined in an interval of 1 week. The average AOM rate of Stage I was calculated based on the AOM rate determined each week. A biomass sample was taken at the end

of this stage for 16S rRNA gene sequencing. In Stage II (Days 48–800), ferrihydrite was periodically added as the sole electron acceptor (Figure 2). Every 3 months, the stirrer was stopped to settle biomass overnight, and 10% of the supernatant (~90 ml, negligible biomass) was replaced with fresh medium. As AOM rate dramatically decreased in this stage, methane was supplied less frequently (every 1–2 months). Gas samples were taken every 3–5 days for methane measurement. Liquid samples were taken every 1–2 weeks for dissolved Fe(II), nitrate, nitrite, ammonium, and acetate measurement. Biomass samples were taken every 1–3 months for 16S rRNA gene sequencing to monitor the shift of the microbial community.

Chemical Analyses

Gaseous methane was measured using a gas chromatograph (GC) (Agilent 7890A, United States) equipped with a HayeSep Q column (mesh size 80/100) (Restek, United States). Dissolved Fe(II) was measured using an Inductively Coupled Plasma-Optical Emission Spectrophotometer (ICP-OES) (PerkinElmer Optima 7300DV, United States). Nitrate, ammonium, and nitrite were measured using a Flow Injection Analyzer (FIA) (Lachat QuickChem8000, United States). Acetate was measured using a GC equipped with a flame ionization detector (PerkinElmer, United States).

DNA Extraction

For DNA extraction, a 0.4 ml biomass sample was used. DNA was isolated using FastDNA Spin Kit for Soil (MP Bio, United States) according to the manufacturer's protocol. The concentration and quality of the extracted DNA were assessed using a Nanodrop spectrophotometer (Thermo Fisher Scientific, United States).

16S rRNA Gene Amplicon Sequencing and Quantitative PCR

The extracted DNA was delivered to the Australian Centre for Ecogenomics (ACE) at The University of Queensland for 16S amplicon sequencing. In addition, the abundance of *Ca. "M. nitroreducens TS"*, methanogens, total bacteria, and total archaea were determined through quantitative PCR (qPCR). The qPCR results were further used for kinetic evaluation of the decay rate of *Ca. "M. nitroreducens TS"*. The details can be found in the Supplementary Material.

Taxonomic Placement, Functional Annotation, and the Construction of the Phylogenomic Tree

DNA samples taken on days 168 and 571 were also used for metagenomic analysis. Library preparation, metagenomic sequencing, quality control, assembly, and binning were described in the Supplementary Material. Phylogeny-based taxonomy was inferred using GTDB-tk version 0.3.2 (with database version r89) (Parks et al., 2018; Chaumeil et al., 2019). The similarity of ANME-associated MAGs with known representatives within the genus *Ca. "Methanoperedens"* was assessed using fastANI version 1.3 (Jain et al., 2018) by calculating pair-wise ANI together with 8 whole-genome sequences from *Ca.*

“Methanoperedens” downloaded from the NCBI Refseq (Pruitt et al., 2007) and Genbank (Benson et al., 2010) databases. Open reading frames (ORFs) were called and annotated using Prokka 1.14.0 (Seemann, 2014). Orthology prediction and additional annotation were carried out using eggno-mapper version 2.0.0 (database version 5.0) (Huerta-Cepas et al., 2017) against Gene Ontology (GO; Consortium, 2004), Kyoto Encyclopedia of Genes and Genomes (KEGG; Kanehisa and Goto, 2000), and clusters of orthologous groups (COG; Koonin, 2002) databases.

A maximum-likelihood phylogenomic tree was constructed using the proteomes of three archaeal MAGs associated with ANME archaea or methanogens together with proteomes of 15 representatives from the genera *Ca.* “Methanoperedens” and *Methanosarcina* were obtained from the NCBI public repository. This was achieved by concatenating 400 universal marker genes in PhyloPhlan3 (Segata et al., 2013), followed by multiple sequence alignment in muscle version 3.8.31 (Edgar, 2004) and tree inference in IQ-TREE version 2.0, with 1,000 bootstrap iterations (Nguyen et al., 2014). The visualization and manual curation of the phylogenomic tree were carried out in interactive tree of life (ITOL; Letunic and Bork, 2006) and Adobe Illustrator.

Identification and Orthology Inference of Multiheme c-Type Cytochromes

C-type cytochromes were first identified from the archaeal proteomes using the “hmmsearch” function of HMMER (version 3.2.1) with the multiheme cytochrome superfamily HMM models (Johnson et al., 2010). They were later confirmed as cytochrome *c* using the BLASTP (Altschul et al., 1997) web service against the NCBI non-redundant (nr) database (updated 05 June 2020). Next, the amount of CXXCH motifs within these cytochromes was determined using the ExPASy web service (Artimo et al., 2012) to search against the PROSITE database (Hulo et al., 2006), and cytochromes containing ≥ 3 CXXCH motifs were retained as MHCs. Afterwards, the cellular allocation of the MHCs was predicted using the SignalP 5.0 (Almagro Armenteros et al., 2019) by identifying signal peptides (SPs) found in transmembrane proteins. Only MHCs with SPs were considered relevant to extracellular electron transport (Leu et al., 2020). To avoid false detection of orthologous genes by naive similarity score-based approaches, orthologous MHCs were identified in three steps by first inferring orthogroups from protein sequences, which were used to infer gene trees, and the gene trees were subsequently used to identify orthologous MHCs. This was done in Orthofinder (version 2.3.12) (Emms and Kelly, 2019).

Assessment of Acetate Metabolism

Four genes are predicted to be critical in acetate consumption, namely, *acd*, encoding acetyl-CoA synthetase (ADP-forming); *acs*, encoding acetyl-CoA synthetase (AMP-forming); *ack*, encoding acetate kinase; and *pta*, encoding phosphotransacetylase (Brown et al., 1977; Bräsen and Schönheit, 2001; Wolfe, 2005). Public proteins of these enzymes were downloaded from the Uniprot database (accessed on 22 February 2020) (The UniProt Consortium, 2017) and were used to create reference packages in GraftM version 0.13.1 (Boyd et al., 2018).

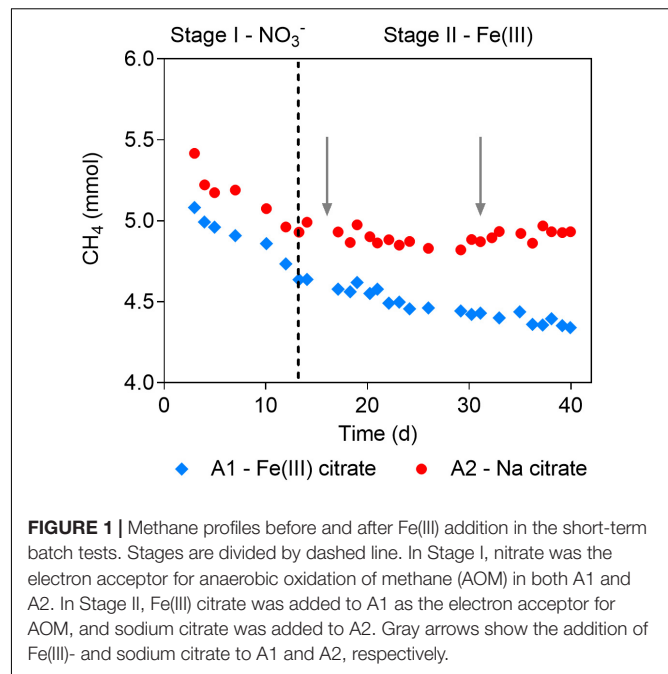


FIGURE 1 | Methane profiles before and after Fe(III) addition in the short-term batch tests. Stages are divided by dashed line. In Stage I, nitrate was the electron acceptor for anaerobic oxidation of methane (AOM) in both A1 and A2. In Stage II, Fe(III) citrate was added to A1 as the electron acceptor for AOM, and sodium citrate was added to A2. Gray arrows show the addition of Fe(III)- and sodium citrate to A1 and A2, respectively.

Later, homologs of *acd*, *acs*, *ack*, and *pta* in the MAGs were revealed using the GraftM “graft” function.

RESULTS

Short-Term Performance of the Culture Using Fe(III) as the Electron Acceptor

In Stage I of the batch tests, obvious methane consumption was observed at similar rates of 368.2 and 406.7 $\mu\text{M day}^{-1}$ in A1 and A2, respectively, when nitrate was served as the electron acceptor (Figure 1). The AOM rates were comparable to that of the parent bioreactor (301.1 $\mu\text{M day}^{-1}$). In Stage II, after nitrate was depleted, methane consumption continued in A1 amended with Fe(III) citrate, although at a lower rate of 103.7 $\mu\text{M day}^{-1}$ (Figure 1). However, no methane consumption was observed in the control group A2 supplied with sodium citrate (Figure 1). These results indicated that *Ca.* “*M. nitroreducens* TS” can sustain AOM by either reducing Fe(III) directly or by coupling to other potential Fe(III)-reducing bacteria *via* direct interspecies electron transfer.

The Long-Term Bioreactor Performance With Ferrihydrite Amendment

In Stage I, methane and nitrate were simultaneously consumed (Figure 2 and Supplementary Figure 1), indicating that AOM was coupled to nitrate reduction. The average AOM rate was 308.6 $\mu\text{M day}^{-1}$. Ammonium was also consumed along with nitrate (Supplementary Figure 1), which suggested that the anammox process occurred. In Stage II, a sharp decrease in the AOM rate was observed immediately after the replacement of nitrate with ferrihydrite (Figure 2). Though one magnitude lower than that in Stage I, methane was still consumed at a rate ranging

from 51.7 to 63.1 $\mu\text{M day}^{-1}$ before day 217, which indicated that AOM occurred in the presence of ferrihydrite. The AOM rate gradually dropped to 11.4 $\mu\text{M day}^{-1}$ on day 464. From day 499 onwards, the AOM rate rebounded and reached 82.0 $\mu\text{M day}^{-1}$ at the end of the incubation. The decrease in the AOM rate between day 551 and day 714 was due to the intensive withdrawal of biomass.

Dissolved Fe(II) production, along with methane consumption, suggested the reduction of ferrihydrite. A previous study has reported that dissolved Fe(II) only accounted for a small fraction (<5%) of the total Fe(II) produced (Cai et al., 2018), which may also be the case in this study. The concentration of dissolved Fe(II) rapidly increased and reached 2.1 mM on day 171, while a sharp drop was observed immediately after each addition of ferrihydrite. A decrease in dissolved Fe(II) was likely due to the absorption of dissolved Fe(II) onto the surface of ferrihydrite (Benjamin and Leckie, 1981; Schultz et al., 1987; Cai et al., 2018). In addition, the peak concentration of dissolved Fe(II) decreased along with the incubation, probably due to the accumulation of solid iron oxides.

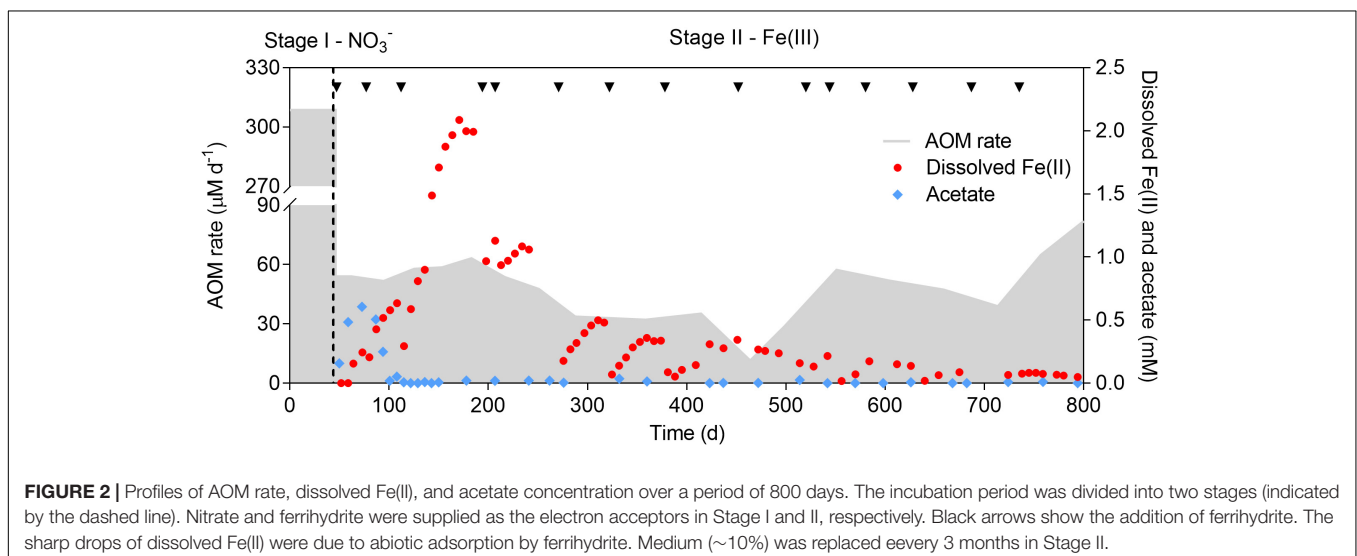
At the beginning of Stage II, acetate was produced after nitrate was depleted, reaching 0.61 mM on day 72 (Figure 2), which was quickly consumed before day 115. Afterward, acetate could only be detected occasionally (<0.04 mM). In Stage II, nitrate was depleted, making the anammox process impossible. Biomass was likely degraded since ammonium was produced (Supplementary Figure 1). Anaerobic ammonium oxidation coupled to Fe(III) reduction (feammox) was reported previously (Huang and Jaffé, 2018). Despite the coexistence of ammonium and ferrihydrite for approximately 750 days, no ammonium consumption was observed (slight decrease in the ammonium concentration was attributed to the dilution by fresh medium) (Supplementary Figure 1). This result indicated that Fe(III) did not serve as an electron acceptor for ammonium oxidation, excluding the contribution of feammox to the production of dissolved Fe(II).

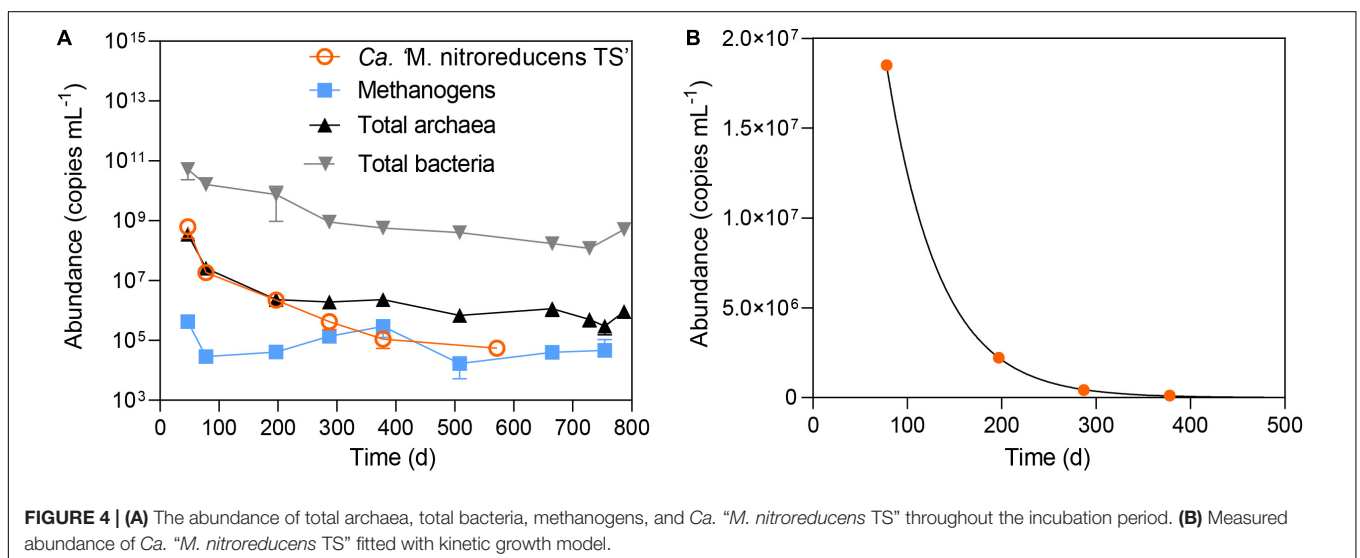
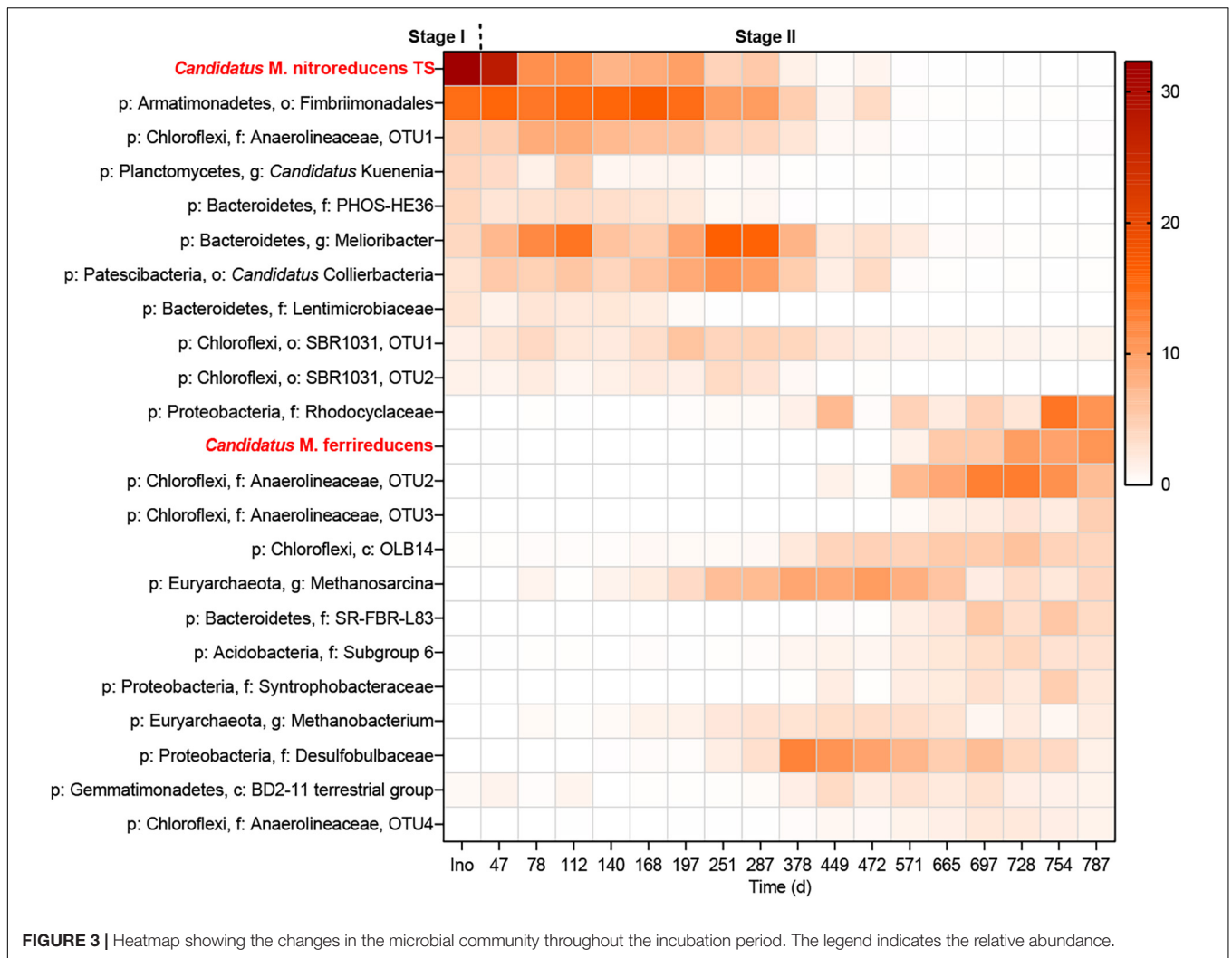
Taken together, continuing methane consumption in conjunction with significant dissolved Fe(II) production

implies that AOM was driven by Fe(III) reduction during the long-term incubation.

Shift in the Microbial Community During the Long-Term Incubation

The microbial community was monitored using 16S rRNA gene amplicon sequencing (Figure 3) and qPCR (Figure 4A). As shown in Figure 3, all the abundant organisms (>1%) in Stage I disappeared at the end of Stage II, while a new community was gradually formed. In Stage I, *Ca. "M. nitroreducens TS"* was highly abundant when nitrate was supplied (relative abundance of 28%), which was similar to that in the parent bioreactor (see the Supplementary Material). In Stage II, switching to ferrihydrite led to a decline in the total amount of microorganisms (Figure 4A) and production of ammonium, indicating biomass degradation. The total bacterial copy numbers dropped from 5.2×10^{10} (day 47) to 1.2×10^8 (day 728) copies ml^{-1} , and the total archaeal copy number decreased from 3.5×10^8 (day 47) to 6.8×10^5 (day 508) copies ml^{-1} . In more than 200 days from the beginning of Stage II, *Ca. "M. nitroreducens TS"* was still abundant, though its relative abundance decreased to 6% on day 287. It further decreased to 0.1% on day 571. This was consistent with the qPCR results, which showed that the copy numbers of *Ca. M. nitroreducens TS* gradually decreased from 6.3×10^8 (day 47) to 5.5×10^4 copies ml^{-1} (day 571) (Figure 4A). In contrast, *Ca. "M. ferrireducens,"* another member of *Ca. "Methanoperedenaceae"* obligate for Fe(III)-dependent AOM (Cai et al., 2018), was detected on day 571. The population of *Ca. "M. ferrireducens"* further increased in the next 200 days and ultimately became abundant (11% on day 787). The copy numbers of total archaea were relatively stable when *Ca. "M. ferrireducens"* was increasing, which indicated that *Ca. "M. ferrireducens"* was enriched in the late period of Stage II. Overall, the abundance of *Ca. "M. nitroreducens TS"* or *Ca. "M. ferrireducens"* was generally in agreement with the AOM rate (Figure 2), indicating that they were responsible for





methane consumption in different periods. The average cellular methane oxidation rate of *Ca. "M. nitroreducens TS"* before day 571 was 7×10^{-16} mol cell⁻¹ day⁻¹, which is comparable to those reported previously (4×10^{-16} to 5×10^{-12} mol cell⁻¹ d⁻¹) (Girguis et al., 2003; Raghoebarsing et al., 2006). Another known anaerobic methanotroph, *Candidatus "Methylomirabilis oxyfera,"* was initially detected at a very low level (0.5%) and was not detected from day 378. Thus, it unlikely contributed to methane consumption. Both 16S sequencing and qPCR results showed that acetotrophic methanogens were enriched before day 378 (Figures 3 and 4A). A batch test supplied with acetate apparently stimulated the growth of a methanogen close to *Methanosarcina mazei* and the production of methane (Supplementary Figure 2).

The relative abundance of *Ca. "K. stuttgartiensis"* declined from 4% to a low level (<0.1%). It indicated that the anammox bacterium was not functioning, which was also supported by the observation of a stable ammonium concentration in the bioreactor. Metal-reducing bacteria belonging to *Geobacter* were only occasionally detected at an exceedingly low level (<0.1%), suggesting that their contribution to Fe(III) reduction was negligible. In contrast, bacteria belonging to the family Rhodocyclaceae were enriched (11% on day 787). Isolation of a Fe(III)-reducing bacterium from this family has been reported (Cummings et al., 1999).

Decay of *Ca. "Methanoperedens nitroreducens TS"* Under the Ferrihydrite Condition

To assess the decay rate of *Ca. "M. nitroreducens TS,"* qPCR readings between day 78 and day 380 were fitted using Equation 3 (Supplementary Material and Figure 4B). It resulted in a decay rate of 0.089 day⁻¹. By comparing to that ($b = 0.002$ day⁻¹) reported previously (He et al., 2013; Chen et al., 2014), the much higher decay rate suggested that the given iron condition was unfavorable to *Ca. "M. nitroreducens TS"*.

Phylogenetic Placement of Key Microorganisms

Two metagenomic-assembled genomes (MAGs) of ANME archaea (bin_27 and bin_53; >95% completeness and <1% contamination) belonging to *Ca. "Methanoperedenaceae"* were recovered from the metagenomes. The genome tree showed that bin_27 formed a cluster with *Ca. "M. nitroreducens TS"* (Haroon et al., 2013) and bin_53 formed another cluster with *Ca. "M. ferrireducens"* (Cai et al., 2018; Figure 5). Further comparison of these two MAGs with their closest relatives (i.e., *Ca. "M. nitroreducens TS"* and *Ca. "M. ferrireducens,"* respectively) showed that the ANI of the two pairs were both close to 100% (Supplementary Figure 3). These results demonstrated that bin_27 and bin_53 were identical to *Ca. "M. nitroreducens TS"* and *Ca. "M. ferrireducens,"* respectively. One MAG (bin_79; >98% completeness and <4% contamination) belonging to methanogen was also retrieved from the metagenomes. The genome tree showed that bin_79

fell into a cluster with *M. mazei* (Youngblut et al., 2015) and shared an ANI of 98%.

Multiheme c-Type Cytochromes and Acetate-Metabolizing Pathways in the Key Microorganisms

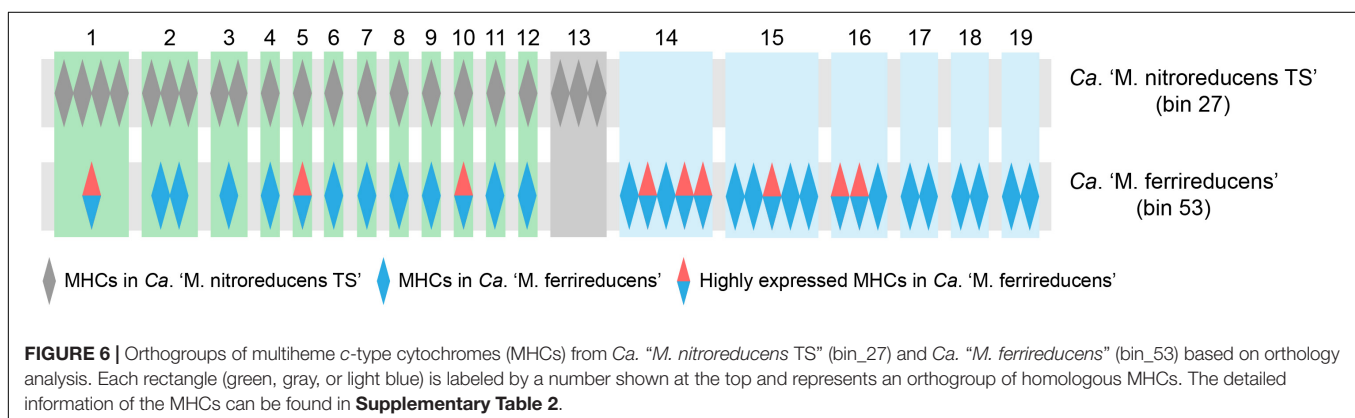
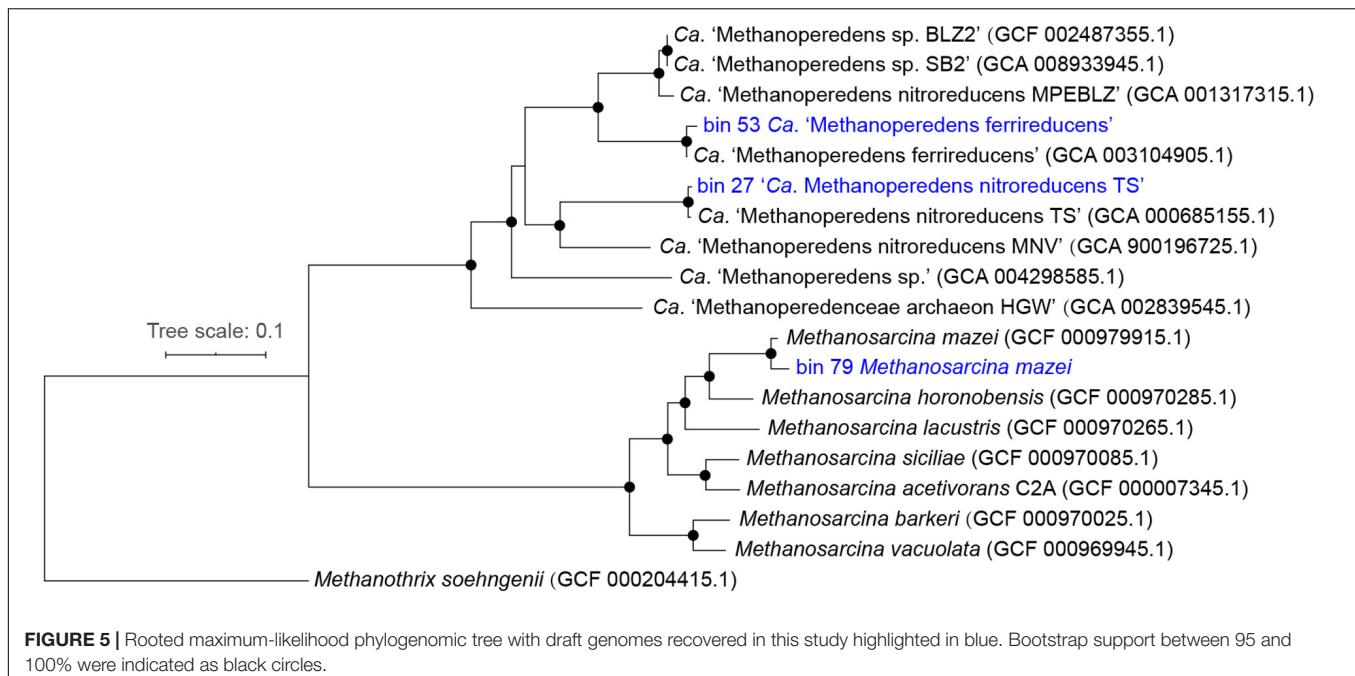
Ca. "M. nitroreducens TS" (bin_27) and *Ca. "M. ferrireducens"* (bin_53) encoded 22 and 36 MHCs, respectively, which were hypothesized to facilitate EET (McGlynn et al., 2015; Cai et al., 2018; Leu et al., 2020). Orthology analysis showed that most of the putative extracellular MHCs from *Ca. "M. nitroreducens TS"* (bin_27) are orthologous to those from *Ca. "M. ferrireducens"* (bin_53), while 19 MHCs are exclusive to *Ca. "M. ferrireducens"* (Figure 6 and Supplementary Table 2). Moreover, 9 MHCs (LAFBCHPI_00375, 01883, 00984, 00699, 02494, 02368, 00697, 00966, and 00967) from *Ca. "M. ferrireducens"* (bin_53) exhibited high expression levels based on the metatranscriptomic data (Cai et al., 2018), which implied that these MHCs were involved in Fe(III) reduction. Notably, three of these highly expressed homologs (LAFBCHPI_00375, 01883, and 00984) were found in *Ca. "M. nitroreducens TS"* (bin_27) (Figure 6 and Supplementary Table 2). Metagenomic analysis also revealed that *M. mazei* (bin_79) possessed one MHC.

In addition, *Ca. "M. nitroreducens TS"* (bin_27) harbored two pathways, i.e., polyhydroxybutyrate (PHB) synthesis pathway and β -oxidation pathway (Eggers and Steinbüchel, 2013; Dibrova et al., 2014; Liu et al., 2016), for PHB metabolism. The PHB synthesis pathway was also found in *Ca. "M. ferrireducens"* (bin_53). *Ca. "M. nitroreducens TS"* (bin_27) and *Ca. "M. ferrireducens"* (bin_53) encoded acetyl-CoA synthetase (Acs/Acd), which is associated with acetate production. *M. mazei* (bin_79) was well-characterized as an acetotrophic methanogen (Westermann et al., 1989), and genes encoding acetate kinase (Ack), phosphate acetyltransferase (Pta), and acetyl-CoA synthase (Acs/Acd) were identified in its genome.

DISCUSSION

Sustaining Fe(III)-Dependent Anaerobic Oxidation of Methane by *Ca. "Methanoperedens nitroreducens TS"* Over a Long-Term Period

This study showed immediate onset of AOM by the *Ca. "M. nitroreducens TS"*-abundant culture in the Fe(III) condition while no methane consumption without Fe(III) (Figure 1). These results supported that *Ca. "M. nitroreducens TS"* can carry out Fe(III)-dependent AOM in nitrate-depleted conditions. It is consistent with the observation of *Ca. "M. nitroreducens MPEBLZ"*, in spite of the large difference in the genomes between these two ANME species (ANI: 77.4%) (Arshad et al., 2015; Ettwig et al., 2016). Motivated by these results, a long-term incubation was conducted to evaluate the response of *Ca. "M. nitroreducens TS"* to Fe(III) amendment. Although



the population kept decreasing after switching from nitrate to ferrihydrite, *Ca. "M. nitroreducens TS"* was the only known methane oxidizer for over 500 days of incubation. In the same period, AOM occurred concomitant with Fe(II) production, though the AOM rate dropped rapidly. These results suggested that *Ca. "M. nitroreducens TS"* sustain a long-term Fe(III)-dependent AOM.

Multiheme c-type cytochromes are ubiquitous in ANME-2 archaea and are hypothetically associated with Fe(III) reduction via EET (Haroon et al., 2013; Wang et al., 2014; McGlynn et al., 2015; Ettwig et al., 2016; Cai et al., 2018; Leu et al., 2020). *Ca. "M. nitroreducens TS"* (bin_27) encodes numerous MHCs, which may facilitate Fe(III) reduction. Until present, direct evidence that MHCs are involved in Fe(III) reduction in ANME archaea is still lacking. Metatranscriptomics analysis of several metal-reducing ANME archaea such as *Ca. "M. ferrireducens"* revealed that some specific MHCs were highly expressed during Fe(III) reduction (Cai et al., 2018; Leu et al., 2020).

Comparison of *Ca. "M. nitroreducens TS"* (bin_27) and *Ca. "M. ferrireducens"* (bin_53) showed that most MHCs from *Ca. "M. nitroreducens TS"* are orthologous to those identified in *Ca. "M. ferrireducens"* (Figure 6). Intriguingly, three of the homologous MHCs were found to be highly expressed in *Ca. "M. ferrireducens"* (Cai et al., 2018). However, whether they are functionally active in *Ca. "M. nitroreducens TS"* still calls for future investigation.

Population Changes in *Ca. "Methanoperedens nitroreducens TS"* and Other Microorganisms

Although *Ca. "M. nitroreducens TS"* drove Fe(III)-dependent AOM for a prolonged period, its population declined based on the results of 16S rRNA gene sequencing, qPCR, and kinetic analysis. The observation that this nitrate-reducing archaeon can reduce Fe(III) is similar to many sulfate-reducing

microorganisms, which grow on sulfate but also can reduce Fe(III) (Jones et al., 1984; Coleman et al., 1993; Lovley, 1993). Those sulfate-reducing bacteria show no growth with Fe(III) as the sole electron acceptor (Lovley et al., 1993). They reduce Fe(III) probably for the following reasons: (1) *c*-type cytochromes as intermediate electron carriers may reduce Fe(III) inadvertently (Lovley et al., 1993); and (2) to facilitate Fe(III) depletion and create a favorable condition for sulfate reduction (Lovley, 2013). These reasons may also apply to *Ca. "M. nitroreducens" TS*. Nonetheless, it should be noted that high concentrations of dissolved Fe(II) and iron precipitates have accumulated in the bioreactor during incubation. The potential adverse effects of these compounds on *Ca. "M. nitroreducens" TS* need further investigation.

Acetate production was observed after switching from nitrate to ferrihydrite (Figure 2). PHB degradation from *Ca. "M. nitroreducens" TS*, which harbors two PHB-metabolizing pathways, may be one of the acetate sources. A previous study has demonstrated that acetate was produced by *Ca. "M. nitroreducens" TS* through limiting the supply of its preferable electron acceptor, i.e., nitrate (Cai et al., 2019). In this study, nitrate was completely removed from the bioreactor, probably creating an unfavorable condition for *Ca. "M. nitroreducens" TS*. Moreover, PHB is a carbon and energy source for many microorganisms (Roohi et al., 2018). Thus, it can be predicted that degradation of PHB may be a strategy for *Ca. "M. nitroreducens" TS* to cope with unfavorable conditions.

In addition, biomass was degraded throughout the incubation, particularly in the early- and mid-phase of Stage II (Figure 4A). Thus, biomass degradation may become another source of acetate and induce Fe(III) reduction by heterotrophic microorganisms. It was estimated that biomass degradation had the potential to contribute to approximately 11–31% Fe(II) formation between days 115 and 337. Bacteria belonging to the family Rhodocyclaceae were abundant in the new community (Figure 3). They are closely related to a denitrifier (*Denitratisoma* sp. strain TSA61) (Ishii et al., 2011); however, it was unlikely that they performed denitrification as no external nitrate or nitrite was fed into the bioreactor. Instead, a representative strain in this family, *Ferribacterium limneticum*, couples Fe(III) reduction to the oxidation of various organic acids such as acetate (Cummings et al., 1999). Therefore, it is hypothesized that these bacteria may use the products of cell lysis, including acetate, for Fe(III) reduction. Acetate may also be used by *M. mazei* for methanogenesis (Supplementary Figure 2).

Environmental Implications

Environments characterized by abundant methane and Fe(III) are prevalent in marine (Beal et al., 2009; Riedinger et al., 2014; Egger et al., 2015) and freshwater systems (Crowe et al., 2011; Sivan et al., 2011; Norđi et al., 2013). Growing studies have suggested that Fe(III)-dependent AOM is a ubiquitous process in those environments, where ANME archaea belongs to family *Ca. "Methanoperedenaceae"* inhabit. For example, the microorganisms were found in freshwater environments, including lake sediments (Weber et al., 2017; Su et al., 2020),

riverbeds (Shen et al., 2019), cryotic thermokarst lakes (Winkel et al., 2019), and saline environments such as submarine permafrost undergoing salt diffusion (Winkel et al., 2018). Beyond that, related 16S rRNA gene sequences were also retrieved from marine settings (Schrenk et al., 2003; Reed et al., 2009). However, the link between Fe(III)-dependent AOM and these ANME archaea in the environment has escaped rigorous investigation (Beal et al., 2009; Crowe et al., 2011; Sivan et al., 2011; Amos et al., 2012; Wankel et al., 2012; Segarra et al., 2013; Riedinger et al., 2014; Egger et al., 2015; Egger et al., 2016; Weber et al., 2016; Egger et al., 2017).

This study shows that *Ca. "M. nitroreducens"* carries out Fe(III)-dependent AOM over a prolonged period, though the AOM rate dropped during the incubation. Coupling methane oxidation to Fe(III) reduction at a recognizable rate implies a potential role of *Ca. "M. nitroreducens"* in biogeochemical cycling of methane and iron. However, it is still puzzling that *Ca. "M. nitroreducens"* did not grow *via* Fe(III)-dependent AOM. Potential adverse conditions such as the toxicity of dissolved Fe(II) (Poulain and Newman, 2009) and overaccumulation of solid iron oxides may prevent the growth of *Ca. "M. nitroreducens"* and should be rigorously tested. In addition, *Ca. "M. nitroreducens"* was initially enriched *via* coupling AOM to nitrate reduction, showing the importance of nitrate in its growth (Haroon et al., 2013). Thus, how *Ca. "M. nitroreducens"* would respond to a co-feeding or interval feeding of nitrate and Fe(III) deserves further investigation.

Moreover, the capability of Fe(III) and nitrate reduction differentiates *Ca. "M. nitroreducens"* from *Ca. "M. ferrireducens,"* which lacks nitrate reductase and may use Fe(III) as its sole electron acceptor (Cai et al., 2018). This difference may have an impact on the distribution of these ANME species in the environment. For instance, nitrate fluctuation is common in many aquatic environments (Weber et al., 2020) and soils (Greenland, 1958), where methane and Fe(III) are also available. It can be speculated that the cooccurrence of Fe(III) and nitrate may create a niche accommodating both *Ca. "M. nitroreducens"* and *Ca. "M. ferrireducens,"* while *Ca. "M. nitroreducens"* may compete with *Ca. "M. ferrireducens"* for Fe(III) when nitrate is not available.

DATA AVAILABILITY STATEMENT

The datasets presented in this study can be found in the online repository: <https://www.ncbi.nlm.nih.gov/bioproject/PRJNA611086> (BioProject accession PRJNA611086; MAG accession SRX8651446, SRX8651447, and SRX8651448).

AUTHOR CONTRIBUTIONS

CC, ZY, and SH conceived and designed the experiments. CC, JX, WL, and JP conducted the experiments. CC, GN, and YZ analyzed the data. CC, GN, YZ, XZ, BH, EM, ZY, and SH interpreted the data. CC and GN wrote

the manuscript. All authors read, reviewed, and approved the submitted version.

FUNDING

This study was funded by the Australian Research Council (ARC) through Project DP170104038, DP180103595, and FL170100086. CC was supported by a Talent Program of Chinese Academy of Sciences (KY2400000012). GN was supported by an Advance Queensland Industry Research Fellowship. JX was supported by The University of Queensland (UQ) Research Training Scholarship. EM was supported by UQ Fellowship. XZ was supported by UQ International Scholarship. WL and JP were supported by China Scholarship Council Scholarship. ZY was a

recipient of an Australian Laureate Fellowship. SH was supported by UQ Amplify Fellowship.

ACKNOWLEDGMENTS

We would like to thank Nathan Clayton and Jianguang Li for chemical analyses.

SUPPLEMENTARY MATERIAL

The Supplementary Material for this article can be found online at: <https://www.frontiersin.org/articles/10.3389/fmicb.2022.799859/full#supplementary-material>

REFERENCES

- Almagro Armenteros, J. J., Tsirigos, K. D., Sønderby, C. K., Petersen, T. N., Winther, O., Brunak, S., et al. (2019). SignalP 5.0 improves signal peptide predictions using deep neural networks. *Nat. Biotechnol.* 37, 420–423. doi: 10.1038/s41587-019-0036-z
- Altschul, S. F., Madden, T. L., Schäffer, A. A., Zhang, J., Zhang, Z., Miller, W., et al. (1997). Gapped BLAST and PSI-BLAST: a new generation of protein database search programs. *Nucleic Acids Res.* 25, 3389–3402. doi: 10.1093/nar/25.17.3389
- Amos, R. T., Bekins, B. A., Cozzarelli, I. M., Voytek, M. A., Kirshstein, J. D., Jones, E. J. P., et al. (2012). Evidence for iron-mediated anaerobic methane oxidation in a crude oil-contaminated aquifer. *Geobiology* 10, 506–517. doi: 10.1111/j.1472-4669.2012.00341.x
- Arshad, A., Speth, D. R., de Graaf, R. M., den Camp, H. J. O., Jetten, M. S., and Welte, C. U. (2015). A metagenomics-based metabolic model of nitrate-dependent anaerobic oxidation of methane by *Methanoperedens*-like archaea. *Front. Microbiol.* 6:1423. doi: 10.3389/fmicb.2015.01423
- Artimo, P., Jonnalagedda, M., Arnold, K., Baratin, D., Csardi, G., de Castro, E., et al. (2012). ExPASy: SIB bioinformatics resource portal. *Nucleic Acids Res.* 40, W597–W603. doi: 10.1093/nar/gks400
- Beal, E. J., House, C. H., and Orphan, V. J. (2009). Manganese- and iron-dependent marine methane oxidation. *Science* 325, 184–187. doi: 10.1126/science.1169984
- Benjamin, M. M., and Leckie, J. O. (1981). Multiple-site adsorption of Cd, Cu, Zn, and Pb on amorphous iron oxyhydroxide. *J. Colloid Interface Sci.* 79, 209–221. doi: 10.1016/0021-9797(81)90063-1
- Benson, D. A., Karsch-Mizrahi, I., Lipman, D. J., Ostell, J., and Sayers, E. W. (2010). GenBank. *Nucleic Acids Res.* 39(suppl. 1), D32–D37.
- Bhattarai, S., Cassarini, C., and Lens, P. N. L. (2019). Physiology and distribution of archaeal methanotrophs that couple anaerobic oxidation of methane with sulfate reduction. *Microbiol. Mol. Biol. Rev.* 83, e00074–e00118. doi: 10.1128/MMBR.00074-18
- Boyd, J. A., Woodcroft, B. J., and Tyson, G. W. (2018). GraftM: a tool for scalable, phylogenetically informed classification of genes within metagenomes. *Nucleic Acids Res.* 46, e59–e59. doi: 10.1093/nar/gky174
- Bräsen, C., and Schönheit, P. (2001). Mechanisms of acetate formation and acetate activation in halophilic archaea. *Arch. Microbiol.* 175, 360–368. doi: 10.1007/s002030100273
- Brown, T. D. K., Jones-Mortimer, M. C., and Kornberg, H. L. (1977). The enzymic interconversion of acetate and acetyl-coenzyme A in *Escherichia coli*. *Microbiology* 102, 327–336. doi: 10.1099/00221287-102-2-327
- Cai, C., Leu, A. O., Xie, G.-J., Guo, J., Feng, Y., Zhao, J.-X., et al. (2018). A methanotrophic archaeon couples anaerobic oxidation of methane to Fe(III) reduction. *ISME J.* 12, 1929–1939. doi: 10.1038/s41396-018-0109-x
- Cai, C., Shi, Y., Guo, J., Tyson, G. W., Hu, S., and Yuan, Z. (2019). Acetate production from anaerobic oxidation of methane via intracellular storage compounds. *Environ. Sci. Technol.* 53, 7371–7379. doi: 10.1021/acs.est.9b00077
- Chaumeil, P.-A., Mussig, A. J., Hugenholtz, P., and Parks, D. H. (2019). GTDB-Tk: a toolkit to classify genomes with the genome taxonomy database. *Bioinformatics* 36, 1925–1927. doi: 10.1093/bioinformatics/btz848
- Chen, X., Guo, J., Shi, Y., Hu, S., Yuan, Z., and Ni, B.-J. (2014). Modeling of simultaneous anaerobic methane and ammonium oxidation in a membrane biofilm reactor. *Environ. Sci. Technol.* 48, 9540–9547. doi: 10.1021/es502608s
- Coleman, M. L., Hedrick, D. B., Lovley, D. R., White, D. C., and Pye, K. (1993). Reduction of Fe(III) in sediments by sulphate-reducing bacteria. *Nature* 361, 436–438. doi: 10.1038/361436a0
- Conrad, R. (2009). The global methane cycle: recent advances in understanding the microbial processes involved. *Environ. Microbiol. Rep.* 1, 285–292. doi: 10.1111/j.1758-2229.2009.00038.x
- Consortium, G. O. (2004). The gene ontology (GO) database and informatics resource. *Nucleic Acids Res.* 32(suppl. 1), D258–D261. doi: 10.1093/nar/gkh036
- Crowe, S., Katsev, S., Leslie, K., Sturm, A., Magen, C., Nomosatryo, S., et al. (2011). The methane cycle in ferruginous Lake Matano. *Geobiology* 9, 61–78. doi: 10.1111/j.1472-4669.2010.00257.x
- Cummings, D. E., Caccavo, F. Jr., Spring, S., and Rosenzweig, R. F. (1999). *Ferribacterium limneticum*, gen. nov., sp. nov., an Fe(III)-reducing microorganism isolated from mining-impacted freshwater lake sediments. *Arch. Microbiol.* 171, 183–188. doi: 10.1007/s002030050697
- Deshpande, T. L., Greenland, D. J., and Quirk, J. P. (1964). Role of iron oxides in the bonding of soil particles. *Nature* 201, 107–108. doi: 10.1016/j.exppara.2019.02.006
- Dibrova, D. V., Galperin, M. Y., and Mulikjanian, A. Y. (2014). Phylogenomic reconstruction of archaeal fatty acid metabolism. *Environ. Microbiol.* 16, 907–918. doi: 10.1111/1462-2920.12359
- Edgar, R. C. (2004). MUSCLE: multiple sequence alignment with high accuracy and high throughput. *Nucleic Acids Res.* 32, 1792–1797. doi: 10.1093/nar/gkh340
- Egger, M., Hagens, M., Sapart, C. J., Dijkstra, N., van Helmond, N. A. G. M., Mogollón, J. M., et al. (2017). Iron oxide reduction in methane-rich deep Baltic sea sediments. *Geochim. Cosmochim. Acta* 207(Suppl C), 256–276. doi: 10.1016/j.gca.2017.03.019
- Egger, M., Kraal, P., Jilbert, T., Sulu-Gambari, F., Sapart, C. J., Röckmann, T., et al. (2016). Anaerobic oxidation of methane alters sediment records of sulfur, iron and phosphorus in the Black sea. *Biogeosciences* 13, 5333–5355. doi: 10.5194/bg-13-5333-2016
- Egger, M., Rasigraf, O., Sapart, C. J., Jilbert, T., Jetten, M. S., Röckmann, T., et al. (2015). Iron-mediated anaerobic oxidation of methane in brackish coastal sediments. *Environ. Sci. Technol.* 49, 277–283. doi: 10.1021/es503663z
- Eggers, J., and Steinbüchel, A. (2013). Poly(3-Hydroxybutyrate) degradation in *Ralstonia eutropha* H16 Is mediated stereoselectively to (S)-3-hydroxybutyryl coenzyme A (CoA) via crotonyl-CoA. *J. Bacteriol.* 195, 3213–3223. doi: 10.1128/JB.00358-13
- Emms, D. M., and Kelly, S. (2019). OrthoFinder: phylogenetic orthology inference for comparative genomics. *Genome Biol.* 20:238. doi: 10.1186/s13059-019-1832-y

- Ettwig, K. F., Butler, M. K., Le Paslier, D., Pelletier, E., Mangenot, S., Kuypers, M. M. M., et al. (2010). Nitrite-driven anaerobic methane oxidation by oxygenic bacteria. *Nature* 464, 543–548. doi: 10.1038/nature08883
- Ettwig, K. F., Zhu, B., Speth, D., Keltjens, J. T., Jetten, M. S., and Kartal, B. (2016). Archaea catalyze iron-dependent anaerobic oxidation of methane. *Proc. Natl. Acad. Sci. U S A* 113, 12792–12796. doi: 10.1073/pnas.1609534113
- Girguis, P. R., Orphan, V. J., Hallam, S. J., and DeLong, E. F. (2003). Growth and methane oxidation rates of anaerobic methanotrophic archaea in a continuous-flow bioreactor. *Appl. Environ. Microbiol.* 69, 5472–5482. doi: 10.1128/AEM.69.9.5472-5482.2003
- Greenland, D. J. (1958). Nitrate fluctuations in tropical soils. *J. Agric. Sci.* 50, 82–92. doi: 10.1017/s0021859600029919
- Haroony, M. F., Hu, S., Shi, Y., Imelfort, M., Keller, J., Hugenholz, P., et al. (2013). Anaerobic oxidation of methane coupled to nitrate reduction in a novel archaeal lineage. *Nature* 500, 567–570. doi: 10.1038/nature12375
- He, Z., Cai, C., Geng, S., Lou, L., Xu, X., Zheng, P., et al. (2013). Modeling a nitrite-dependent anaerobic methane oxidation process: parameters identification and model evaluation. *Bioresour. Technol.* 147, 315–320. doi: 10.1016/j.biortech.2013.08.001
- Hinrichs, K., and Boetius, A. (2002). “The anaerobic oxidation of methane: new insights in microbial ecology and biogeochemistry,” in *Ocean Margin Systems*, eds G. Wefer, D. Billett, D. Hebeln, B. Jørgensen, M. Schlüter, T. Van Weering, (Heidelberg: Springer-Verlag), 457–477. doi: 10.1007/978-3-662-05127-6_28
- Hu, B.-I., Shen, L.-d., Lian, X., Zhu, Q., Liu, S., Huang, Q., et al. (2014). Evidence for nitrite-dependent anaerobic methane oxidation as a previously overlooked microbial methane sink in wetlands. *Proc. Natl. Acad. Sci. U S A* 111, 4495–4500. doi: 10.1073/pnas.1318393111
- Huang, S., and Jaffé, P. R. (2018). Isolation and characterization of an ammonium-oxidizing iron reducer: Acidimicrobiaceae sp. A6. *PLoS One* 13:e0194007. doi: 10.1371/journal.pone.0194007
- Huerta-Cepas, J., Forslund, K., Coelho, L. P., Szklarczyk, D., Jensen, L. J., von Mering, C., et al. (2017). Fast genome-wide functional annotation through orthology assignment by eggNOG-mapper. *Mol. Biol. Evol.* 34, 2115–2122. doi: 10.1093/molbev/msx148
- Hulo, N., Bairoch, A., Bulliard, V., Cerutti, L., De Castro, E., Langendijk-Genevaux, P. S., et al. (2006). The prosite database. *Nucleic Acids Res.* 34(suppl. 1), D227–D230.
- In ‘t Zandt, M. H., de Jong, A. E. E., Slomp, C. P., and Jetten, M. S. M. (2018). The hunt for the most-wanted chemolithoautotrophic spookmicrobes. *FEMS Microbiol. Ecol.* 94, fiy064–fiy064. doi: 10.1093/femsec/fiy064
- Ishii, S., Ashida, N., Otsuka, S., and Senoo, K. (2011). Isolation of oligotrophic denitrifiers carrying previously uncharacterized functional gene sequences. *Appl. Environ. Microbiol.* 77, 338–342. doi: 10.1128/AEM.02189-10
- Jain, C., Rodriguez-R, L. M., Phillippy, A. M., Konstantinidis, K. T., and Aluru, S. (2018). High throughput ANI analysis of 90K prokaryotic genomes reveals clear species boundaries. *Nat. Commun.* 9:5114.
- Johnson, L. S., Eddy, S. R., and Portugaly, E. (2010). Hidden Markov model speed heuristic and iterative HMM search procedure. *BMC Bioinformatics* 11:431. doi: 10.1186/1471-2105-11-431
- Jones, J. G., Davison, W., and Gardener, S. (1984). Iron reduction by bacteria: range of organisms involved and metals reduced. *FEMS Microbiol. Lett.* 21, 133–136. doi: 10.1111/j.1574-6968.1984.tb00198.x
- Kanehisa, M., and Goto, S. (2000). KEGG: kyoto encyclopedia of genes and genomes. *Nucleic Acids Res.* 28, 27–30.
- Knittel, K., and Boetius, A. (2009). Anaerobic oxidation of methane: progress with an unknown process. *Annu. Rev. Microbiol.* 63, 311–334. doi: 10.1146/annurev.micro.61.080706.093130
- Koonin, E. V. (2002). “The Clusters of Orthologous Groups (COGs) database: phylogenetic classification of proteins from complete genomes,” in *The NCBI Handbook*, eds J. McEntyre and J. Ostell (Bethesda, MD: National Center for Biotechnology Information).
- Letunic, I., and Bork, P. (2006). Interactive tree of life (iTOL): an online tool for phylogenetic tree display and annotation. *Bioinformatics* 23, 127–128. doi: 10.1093/bioinformatics/btl529
- Leu, A. O., Cai, C., McLroy, S. J., Southam, G., Orphan, V. J., Yuan, Z., et al. (2020). Anaerobic methane oxidation coupled to manganese reduction by members of the Methanoperedenaceae. *ISME J.* 14, 1030–1041. doi: 10.1038/s41396-020-0590-x
- Li, W., Cai, C., Song, Y., Ni, G., Zhang, X., and Lu, P. (2021). The role of crystalline iron oxides in methane mitigation through anaerobic oxidation of methane. *ACS ES&T Water* 1, 1153–1160. doi: 10.1021/acestwater.0c00199
- Liu, G., Cai, S., Hou, J., Zhao, D., Han, J., Zhou, J., et al. (2016). Enoyl-CoA hydratase mediates polyhydroxyalkanoate mobilization in *Haloferax mediterranei*. *Sci. Rep.* 6:24015. doi: 10.1038/srep24015
- Lovley, D. (2013). in *The Prokaryotes: Prokaryotic Physiology and Biochemistry*, eds E. Rosenberg, E. F. DeLong, S. Lory, E. Stackebrandt, and F. Thompson (Heidelberg: Springer), 287–308.
- Lovley, D. R. (1993). Dissimilatory metal reduction. *Annu. Rev. Microbiol.* 47, 263–290. doi: 10.1146/annurev.mi.47.100193.001403
- Lovley, D. R., Giovannoni, S. J., White, D. C., Champagne, J. E., Phillips, E. J. P., Gorby, Y. A., et al. (1993). *Geobacter metallireducens* gen. nov. sp. nov., a microorganism capable of coupling the complete oxidation of organic compounds to the reduction of iron and other metals. *Arch. Microbiol.* 159, 336–344. doi: 10.1007/BF00290916
- Martin, J.-M., and Meybeck, M. (1979). Elemental mass-balance of material carried by major world rivers. *Mar. Chem.* 7, 173–206. doi: 10.1016/j.scitotenv.2008.09.053
- McGlynn, S. E., Chadwick, G. L., Kempes, C. P., and Orphan, V. J. (2015). Single cell activity reveals direct electron transfer in methanotrophic consortia. *Nature* 526, 531–535. doi: 10.1038/nature15512
- Meyerdieks, A., Kube, M., Kostadinov, I., Teeling, H., Glöckner, F. O., Reinhardt, R., et al. (2010). Metagenome and mRNA expression analyses of anaerobic methanotrophic archaea of the ANME-1 group. *Environ. Microbiol.* 12, 422–439. doi: 10.1111/j.1462-2920.2009.02083.x
- Nguyen, L.-T., Schmidt, H. A., von Haeseler, A., and Minh, B. Q. (2014). IQ-TREE: a fast and effective stochastic algorithm for estimating maximum-likelihood phylogenies. *Mol. Biol. Evol.* 32, 268–274. doi: 10.1093/molbev/msu300
- Noröi, K. A., Thamdrup, B., and Schubert, C. J. (2013). Anaerobic oxidation of methane in an iron-rich Danish freshwater lake sediment. *Limnol. Oceanogr.* 58, 546–554. doi: 10.4319/lo.2013.58.2.0546
- Parks, D. H., Chuvochina, M., Waite, D. W., Rinke, C., Skarshewski, A., Chaumeil, P.-A., et al. (2018). A standardized bacterial taxonomy based on genome phylogeny substantially revises the tree of life. *Nat. Biotechnol.* 36, 996–1004. doi: 10.1038/nbt.4229
- Poulain, A. J., and Newman, D. K. (2009). *Rhodobacter capsulatus* catalyzes light-dependent Fe(II) oxidation under anaerobic conditions as a potential detoxification mechanism. *Appl. Environ. Microbiol.* 75, 6639–6646. doi: 10.1128/AEM.00054-09
- Pruitt, K. D., Tatusova, T., and Maglott, D. R. (2007). NCBI reference sequences (RefSeq): a curated non-redundant sequence database of genomes, transcripts and proteins. *Nucleic Acids Res.* 35, D61–D65. doi: 10.1093/nar/gkl842
- Raghoebarsing, A. A., Pol, A., van de Pas-Schoonen, K. T., Smolders, A. J. P., Ettwig, K. F., Rijpstra, W. I. C., et al. (2006). A microbial consortium couples anaerobic methane oxidation to denitrification. *Nature* 440, 918–921. doi: 10.1038/nature04617
- Reeburgh, W. S. (2007). Oceanic methane biogeochemistry. *Chem. Rev.* 107, 486–513. doi: 10.1021/cr050362v
- Reed, A. J., Dorn, R., Van Dover, C. L., Lutz, R. A., and Vetriani, C. (2009). Phylogenetic diversity of methanogenic, sulfate-reducing and methanotrophic prokaryotes from deep-sea hydrothermal vents and cold seeps. deep sea research part II. *Top. Stud. Oceanogr.* 56, 1665–1674. doi: 10.1016/j.dsr.2.2009.05.012
- Riedinger, N., Formolo, M. J., Lyons, T. W., Henkel, S., Beck, A., and Kasten, S. (2014). An inorganic geochemical argument for coupled anaerobic oxidation of methane and iron reduction in marine sediments. *Geobiology* 12, 172–181. doi: 10.1111/gbi.12077
- Roohi, Zaheer, M. R., and Kuddus, M. (2018). PHB (poly-β-hydroxybutyrate) and its enzymatic degradation. *Polym. Adv. Technol.* 29, 30–40. doi: 10.1002/pat.4126
- Scheller, S., Yu, H., Chadwick, G. L., McGlynn, S. E., and Orphan, V. J. (2016). Artificial electron acceptors decouple archaeal methane oxidation from sulfate reduction. *Science* 351, 703–707. doi: 10.1126/science.1247154
- Schrenk, M. O., Kelley, D. S., Delaney, J. R., and Baross, J. A. (2003). Incidence and diversity of microorganisms within the walls of an active deep-sea sulfide

- chimney. *Appl. Environ. Microbiol.* 69, 3580–3592. doi: 10.1128/AEM.69.6.3580-3592.2003
- Schultz, M. F., Benjamin, M. M., and Ferguson, J. F. (1987). Adsorption and desorption of metals on ferrihydrite: reversibility of the reaction and sorption properties of the regenerated solid. *Environ. Sci. Technol.* 21, 863–869. doi: 10.1021/es00163a003
- Seemann, T. (2014). Prokka: rapid prokaryotic genome annotation. *Bioinformatics* 30, 2068–2069. doi: 10.1093/bioinformatics/btu153
- Segarra, K. E., Schubotz, F., Samarkin, V., Yoshinaga, M. Y., Hinrichs, K. U., and Joye, S. B. (2015). High rates of anaerobic methane oxidation in freshwater wetlands reduce potential atmospheric methane emissions. *Nat. Commun.* 6:7477. doi: 10.1038/ncomms8477
- Segarra, K. E. A., Comerford, C., Slaughter, J., and Joye, S. B. (2013). Impact of electron acceptor availability on the anaerobic oxidation of methane in coastal freshwater and brackish wetland sediments. *Geochim. Cosmochim. Acta* 115, 15–30. doi: 10.1016/j.gca.2013.03.029
- Segata, N., Börnigen, D., Morgan, X. C., and Huttenhower, C. (2013). PhyloPhlAn is a new method for improved phylogenetic and taxonomic placement of microbes. *Nat. Commun.* 4:2304. doi: 10.1038/ncomms3304
- Shen, L.-D., Ouyang, L., Zhu, Y., and Trimmer, M. (2019). Active pathways of anaerobic methane oxidation across contrasting riverbeds. *ISME J.* 13, 752–766. doi: 10.1038/s41396-018-0302-y
- Shi, L., Dong, H., Reguera, G., Beyenal, H., Lu, A., Liu, J., et al. (2016). Extracellular electron transfer mechanisms between microorganisms and minerals. *Nat. Rev. Microbiol.* 14, 651–662. doi: 10.1038/nrmicro.2016.93
- Shi, L., Squier, T. C., Zachara, J. M., and Fredrickson, J. K. (2007). Respiration of metal (hydr)oxides by *Shewanella* and *Geobacter*: a key role for multiheme c-type cytochromes. *Mol. Microbiol.* 65, 12–20. doi: 10.1111/j.1365-2958.2007.05783.x
- Sivan, O., Adler, M., Pearson, A., Gelman, F., Bar-Or, I., John, S. G., et al. (2011). Geochemical evidence for iron-mediated anaerobic oxidation of methane. *Limnol. Oceanogr.* 56, 1536–1544.
- Su, G., Zopfi, J., Yao, H., Steinle, L., Niemann, H., and Lehmann, M. F. (2020). Manganese/iron-supported sulfate-dependent anaerobic oxidation of methane by archaea in lake sediments. *Limnol. Oceanogr.* 65, 863–875. doi: 10.1002/lno.11354
- The UniProt Consortium (2017). UniProt: the universal protein knowledgebase. *Nucleic Acids Res.* 45, D158–D169.
- Topp, E., and Pattey, E. (1997). Soils as sources and sinks for atmospheric methane. *Can. J. Soil Sci.* 77, 167–177. doi: 10.4141/s96-107
- Wang, F.-P., Zhang, Y., Chen, Y., He, Y., Qi, J., Hinrichs, K.-U., et al. (2014). Methanotrophic archaea possessing diverging methane-oxidizing and electron-transporting pathways. *ISME J.* 8, 1069–1078. doi: 10.1038/ismej.2013.212
- Wankel, S. D., Adams, M. M., Johnston, D. T., Hansel, C. M., Joye, S. B., and Girguis, P. R. (2012). Anaerobic methane oxidation in metalliferous hydrothermal sediments: influence on carbon flux and decoupling from sulfate reduction. *Environ. Microbiol.* 14, 2726–2740. doi: 10.1111/j.1462-2920.2012.02825.x
- Weber, G., Honecker, U., and Kubiniok, J. (2020). Nitrate dynamics in springs and headwater streams with agricultural catchments in southwestern Germany. *Sci. Total Environ.* 722:137858. doi: 10.1016/j.scitotenv.2020.137858
- Weber, H. S., Habicht, K. S., and Thamdrup, B. (2017). Anaerobic methanotrophic archaea of the anme-2d cluster are active in a low-sulfate, iron-rich freshwater sediment. *Front. Microbiol.* 8:619. doi: 10.3389/fmicb.2017.00619
- Weber, H. S., Thamdrup, B., and Habicht, K. S. (2016). High sulfur isotope fractionation associated with anaerobic oxidation of methane in a low-sulfate, iron-rich environment. *Front. Earth Sci.* 4:61. doi: 10.3389/feart.2016.00061
- Welte, C. U., Rasigraf, O., Vaksmaa, A., Versantvoort, W., Arshad, A., Op den Camp, H. J. M., et al. (2016). Nitrate- and nitrite-dependent anaerobic oxidation of methane. *Environ. Microbiol. Rep.* 8, 941–955. doi: 10.1111/1758-2229.12487
- Westermann, P., Ahring, B. K., and Mah, R. A. (1989). Threshold acetate concentrations for acetate catabolism by aceticlastic methanogenic bacteria. *Appl. Environ. Microbiol.* 55, 514–515. doi: 10.1128/aem.55.2.514-515.1989
- Winkel, M., Mitzscherling, J., Overduin, P. P., Horn, F., Winterfeld, M., Rijkers, R., et al. (2018). Anaerobic methanotrophic communities thrive in deep submarine permafrost. *Sci. Rep.* 8:1291. doi: 10.1038/s41598-018-19505-9
- Winkel, M., Sepulveda-Jauregui, A., Martinez-Cruz, K., Heslop, J. K., Rijkers, R., Horn, F., et al. (2019). First evidence for cold-adapted anaerobic oxidation of methane in deep sediments of thermokarst lakes. *Environ. Res. Commun.* 1:021002. doi: 10.1088/2515-7620/ab1042
- Wolfe, A. J. (2005). The acetate switch. *Microbiol. Mol. Biol. Rev.* 69, 12–50. doi: 10.1128/mmbr.69.1.12-50.2005
- Youngblut, N. D., Wirth, J. S., Henriksen, J. R., Smith, M., Simon, H., Metcalf, W. W., et al. (2015). Genomic and phenotypic differentiation among *Methanosarcina mazei* populations from Columbia river sediment. *ISME J.* 9, 2191–2205.

Conflict of Interest: The authors declare that the research was conducted in the absence of any commercial or financial relationships that could be construed as a potential conflict of interest.

Publisher's Note: All claims expressed in this article are solely those of the authors and do not necessarily represent those of their affiliated organizations, or those of the publisher, the editors and the reviewers. Any product that may be evaluated in this article, or claim that may be made by its manufacturer, is not guaranteed or endorsed by the publisher.

Copyright © 2022 Cai, Ni, Xia, Zhang, Zheng, He, Marcellin, Li, Pu, Yuan and Hu. This is an open-access article distributed under the terms of the Creative Commons Attribution License (CC BY). The use, distribution or reproduction in other forums is permitted, provided the original author(s) and the copyright owner(s) are credited and that the original publication in this journal is cited, in accordance with accepted academic practice. No use, distribution or reproduction is permitted which does not comply with these terms.